Hierarchical approach for fusion of electroencephalography and electromyography for predicting finger movements and kinematics using deep learning

by Prihartini Widiyanti

Submission date: 19-May-2023 01:00PM (UTC+0800)
Submission ID: 2096826886
File name: Januari_2023_-_Neurocomputing_Fusion_of_EEG_and_EMG.pdf (3.25M)
Word count: 10017
Character count: 53839

Neurocomputing 527 (2023) 184–195

Contents lists available at ScienceDirect

Neurocomputing

journal homepage: www.elsevier.com/locate/neucom

Hierarchical approach for fusion of electroencephalography and electromyography for predicting finger movements and kinematics using deep learning

Tanaya Das [a], Lakhyajit Gohain [a], Nayan M Kakoty [a], MB Malarvili [b], Prihartini Widiyanti [c], Gajendra Kumar [d,*]

[a] Embedded Systems and Robotics Lab, School of Engineering, Tezpur University, India
[b] Faculty of Bioscience and Medical Engineering, Universiti Teknologi Malaysia, Malaysia
[c] Faculty of Science and Technology, Universitas Airlangga, Indonesia
[d] Department of Neuroscience, City University of Hong Kong, Tat Chee Avenue, Hong Kong Special Administrative Region

ARTICLE INFO

Article history:
Received 6 January 2022
Revised 23 December 2022
Accepted 9 January 2023
Available online 13 January 2023
Communicated by Zidong Wang

Keywords:
Electroencephalography
Electromyography
Artificial intelligence
Brain-computer interface
Hierarchical
Finger Kinematics
Finger Movements

ABSTRACT

The brain is a unique organ that performs multiple processes simultaneously, such as sensory, motor, and cognitive function. However, several neurological diseases (ataxia, dystonia, Huntington's disease) or trauma affect the limb movement and there is no cure. Although brain-computer interfaces (BCIs) have been recently used to improve the quality of life for people with severe motor disabilities, anthropomorphic control of a prosthetic hand in upper limb rehabilitation still remains an unachieved goal. To this purpose, a hierarchical integration of neural commands to fingers was applied for execution of human hand grasping with better precision. For finger movement prediction and kinematics estimation, a neuromuscular approach was employed to establish a hierarchical synergy between electroencephalography (EEG) and electromyography (EMG). EEG, EMG and metacarpophalangeal (MCP) joint kinematics were acquired during five finger flexion movements of the human hand. EMG for five finger movements and kinematics were estimated from EEG using linear regression. A Long Short-Term Memory network (LSTM) and a random forest regressor were adjoined hierarchically for prediction of finger movements and estimation of finger kinematics from the estimated EMG. The results showed an average accuracy of 84.25 ± 0.61 % in predicting finger movements and an average minimum error of 0.318 ± 0.011 in terms of root mean squared error (RMSE) in predicting finger kinematics from EEG across six subjects and five fingers. These findings suggest the implementation of a hierarchical approach to develop anthropomorphic control for upper limb prostheses.

1. Introduction

57.7 million traumatic non-fatal limb amputation occur worldwide [1] requiring partial or complete surgical removal of limb or extremity such as an arm, leg, foot, hand, toe, or finger. Absence of anatomical structures due to amputations negatively affects psychology and body functions such as mobility. Prosthesis and rehabilitation are being commonly used to improve the quality of people's life in such cases using electroencephalography (EEG) and electromyography (EMG) for their non-invasive signal acquisition and an abundance of synchronized neuronal information [2]. Prediction of upper limb movements using EEG and EMG has been mostly applied to control limb prosthesis and rehabilitation [3]. Several recent studies have reported interactions of EEG with the performance of upper limb prosthetics devices [4], upper limb reaching tasks [5], and finger movements [6]. However, limited studies have been reported for estimation of EMG from EEG to predict upper limb movements and kinematics. EMG estimation from EEG to predict finger movements and finger kinematics will aid in developing control of robotic limb prostheses and rehabilitation for amputees as they generate minimal EMG [7]. Cho et al. [8] reported a 63.89 % prediction accuracy for natural grasp movements based on muscle activity patterns, estimated from EEG using a linear discriminant analysis (LDA) model. The studies confirm the benefit of

* Corresponding author at: Department of Molecular Biology, Cell Biology & Biochemistry (MCB), Brown University, 70 Ship Street, Providence, RI, 02906. Phone: (+401) 499-6970.
E-mail addresses: tanaya12das@gmail.com (T. Das), lakhya25@gmail.com (L. Gohain), nkakoty@tezu.ernet.in (N.M Kakoty), gajendra_kumar@brown.edu (G. Kumar).

https://doi.org/10.1016/j.neucom.2023.01.061
0925-2312/

EEG to control finger kinematics for grasping through brain-computer interfaces (BCIs). However, artificial intelligence (AI) is required to train large amounts of labelled data to enhance the precision. Application of BCIs with AI has been recently investigated in clinics to achieve real-time modulation and feedback [9]. Algorithms modulates the decision based on the previous set of data. Therapeutic intervention in stroke patients showed partial regaining of function in the affected limb. A closed loop system between cortical activity and movement, mimics the afferent feedback to restore functional corticospinal and corticomuscular connections [10]. Clinical application of BCI with AI are still very limited due to disparity in prediction and interpretation of real-world activity, which can be improved by using deep learning techniques. Recently, BCI applications with AI assistance have advanced the analysis and decoding of brain signals, as well as the ability to execute real-time hand movements [10,11]. However, the performance of BCI with AI using EEG for prediction of finger movements and estimation of finger kinematics remains elusive. Integration of AI with BCI has revolutionized the field of machine learning through the advancement of deep learning, thereby decreasing the error rate, processing large amounts of data and maximizing performance by performing self trials and errors [12,13]. The AI-BCI architecture holds promise to improve the clinical reliability of BCI performance in touch with EEG by enhancing the AI key metric with the BCI architecture. Movement of a human hand requires complex motor patterns by coordinating the responses of multiple muscles. EEG and EMG have been used to decode the intention to move the hand [14–16] using BCIs, with EEG playing a vital role in the control of prosthetic limbs in amputees [17]. BCIs integrate robotic systems with brain signals, allowing for intuitive control of neuro-prostheses such as robotic arms and actively generating a movement or imagining motor actions [18].

This study proposes a novel strategy for finger movement prediction and kinematics estimation from EEG and EMG by utilizing a hybrid BCI system. To predict finger movement and kinematics, a hierarchical approach strategy comprising EEG and EMG fusion attained through estimation of EMG from EEG with AI techniques was used. Data from 18-channel EEG, 4-channel EMG and metacarpophalangeal (MCP) joint angles during right hand flexion of five fingers was acquired and used for the experiment. Fusion of information has been used in many studies to achieve better performance for a desired task. Tang et al. [19] proposed a Y-shape dynamic Transformer (YDTR) method based on fusion of infrared and visible image information to attain superior performance and better generalization ability. Tang et al. [20] further reported a multiscale adaptive transformer model fusing multimodal medical images to achieve better clinical diagnosis and surgical navigation. Leon-Garza et al. [21] used a type-2 based fuzzy logic system approach for fusion of 2D digital information into creating a 3D BIM model to attain an augmentable and interpretable model. The studies demonstrate the benefit of combining different information for a task. As such, the proposed study also aims to achieve better accuracy for predicting finger movement and kinematics using hierarchical fusion of EMG and EEG. Application of hierarchical approach represents sub-networks of EEG-based signal recognition, EMG decoding from EEG, and BCI system integration with AI impartment. Proposed work thus skillfully combines several concepts, approaches, techniques and components such as EEG, EMG, BCI, AI, finger movements and finger kinematics. The estimation of EMG from EEG is advantageous for developing control of hand prostheses and robotic exoskeletons in individuals with hand impairment as they generate little to no EMG due to insufficient muscle strength. Further, since the motor cortex region is the main source of movement and grasping, decoding muscle signals (EMG) from cortical signals (EEG) would also be beneficial.

Simultaneous prediction of finger movements and kinematics from the estimated EMG with AI techniques contributes to a more intuitive and natural movement as well as grasp control in a prosthetic or exoskeleton hand for rehabilitation. Additionally, the use of deep learning architectures and regression models allows for high precision and accuracy in the neurorehabilitation process. The methods dissect the mechanism of motor deficits caused by pathological brain changes. Furthermore, it helps to customize the therapies by supporting the clinicians with relevant data on motor organization. The reported work has been further tested to control individual finger movements of an indigenously developed sensorized prosthetic hand. The study being implemented intends to develop anthropomorphic control for upper limb prostheses, that can be utilized in clinical settings.

The remainder of this paper is organized as follows: Section 2 describes materials and methods for subject preparation, hardware implementation, software implementation, experimental setup with data collection and experimental protocol. Section 3 presents experimental results and discussion including signal preprocessing as well as movement and kinematics prediction framework. Section 4 summarizes conclusion of the study.

2. Materials and methods

2.1. Subjects

Six healthy volunteers (4 males and 2 females) with a mean age of 26.5 ± 4 years took part in the experiment. The study was approved by the institutional ethics committee of Tezpur University, India. Written consent according to the Helsinki declaration [22] was obtained from each subject. All participants were right-handed and had no known neurological or muscular disorders. Experimental protocol was demonstrated to the participants before the start of the experiment.

2.2. Hardware implementation

2.2.1. NS-EEG-D1 system

NS-EEG-D1 system from Neurostyle (Neurostyle PTE ltd, Hill View, Singapore) was used for the acquisition of EEG. The system provided up to 64 channels of EEG recordings, built-in impedance testing, and synchronous acquisition with other physiological signals. It comprised of an EEG cap with electrodes affixed according to the 10–20 international standard as well as cables for connecting the system to power supply and laptop. Important technical specifications of the system are listed in Table S9 (Supplementary Material).

2.2.2. Shield-EKG-EMG

Four SHIELD-EKG-EMG boards from Olimex were stacked on top of one another and interfaced with an Arduino UNO for acquisition of 4-channel EMG. Inputs attached to shield, picks the analog differential signal generated by the muscles while the shield converts it into a single stream of output data. To discretize the signal, ADC embedded in the microcontroller of Arduino UNO further converts the analog signal to a digital signal. The shield has an inbuilt instrumentation amplifier and a Besselworth filter with a cut-off 40 Hz. The total gain of the shield is 2848. A SHIELD-EKG-EMG board is shown in Figure S5 (Supplementary Material).

2.2.3. Arduino Uno

Arduino Uno was used with the SHIELD-EKG-EMG boards for the acquisition of 4-channel EMG and acquisition of kinematic data from a data glove. The SHIELD-EKG-EMG boards were mounted on one another with Arduino Uno as the base board. Connectors on

the SHIELD-EKG-EMG, adhered to the Arduino Uno interfacing specifications.

2.2.4. Ag-AgCl electrodes

Pre-gelled disposable Ag-AgCl electrodes of 1 cm in diameter from 3 M were used for EMG acquisition by placing them over the area of target muscles. An important feature of these electrodes was that they were single use and hygienic. Connection between electrodes to shield boards was made through four lead cables.

2.2.5. Data glove

A right-hand standard gardener's glove customized with five flex sensors, one per finger was utilised for the acquisition of kinematic data. It was interfaced with an Arduino Uno for data acquisition. The data glove equipped with flex sensors is shown in Figure S6.

2.2.6. Flex sensors

Five flex sensors of 2.2 in. from Spectra Symbol were attached to the data glove to collect kinematic data of five fingers. The sensors were calibrated to collect data for flexion of MCP joint angles of each finger.

2.3. Software implementation

2.3.1. Arduino IDE

Arduino IDE is an integrated development environment (IDE), required for writing and uploading code to Arduino board. The code for acquisition of EMG and kinematic data was written in Arduino IDE Windows version 1.6.11 and uploaded to an Arduino Uno board.

2.3.2. NS-EEG software

NS-EEG software version 19 was used to record, store, and visualise EEG data. The software assisted in selecting EEG montages required for the experiment, automatic impedance checking, storing subjects' databases, visualizing and analysing the data.

2.3.3. Spyder (Anaconda)

Spyder (Scientific Python Development Environment), a free and open-source python-based scientific development environment (IDE), was used for coding and implementing the machine learning and deep learning models presented in this work. Spyder's built-in integrated libraries, such as NumPy, Pandas, SciPy, and Matplotlib, were used in preparing and pre-processing the dataset using Python 3.7. Also, Scikit Learn and Tensorflow 2.0 with Keras 2.4.1 libraries were used to develop the proposed models for the hierarchical approach.

2.4. Experimental setup and data collection

Experimental setup was comprised of an EMG acquisition system, an EEG acquisition system, and a data glove as shown in Fig. 1A. SHIELD-EKG-EMG boards were used for the acquisition of 4-channel EMG from each subject. Disposable pre-gelled Ag-AgCl surface electrodes were placed in a bipolar setting, keeping an inter-electrode distance of 20 mm over the area of target muscles of the subjects. Skin covering the area of target muscles was cleaned with isopropyl alcohol before placing the electrodes. Lead cables were connected to the electrodes and SHIELD-EKG-EMG board for EMG acquisition. The target muscles with their corresponding finger movements and flexed joints are listed in Table S1. All channels had a common reference at the right elbow. The EMG data was acquired at a sampling rate of 512 Hz from the shield using Arduino Uno with a 10-bit analog-to-digital (A/D) converter. The shield has an inbuilt amplifier and bandpass filter to remove noise. EMG acquired were visualized in real-time to ensure quality of the signals during acquisition.

Kinematics of finger movements was acquired simultaneously with EMG, from right hand of the subjects using the data glove equipped with five flex sensors. The data glove was calibrated to collect data on the MCP joint angles for each finger of the right hand. These data was recorded at a sampling rate of 100 Hz. Later in the data pre-processing step, cubic interpolation was performed to fix the sampling rate at 512 Hz, so as to keep it synchronized with that of the EMG and EEG data.

EEG data was recorded simultaneously with EMG and finger kinematics using Neurostyle's NS-EEG-D1 system from 22 monopolar channels fixed to an EEG electrode cap according to the international 10–20 standards [23]. The selected channels included Fp1, Fp2, F3, F4, C3, C4, P3, P4, O1, O2, F7, F8, T3, T4, T5, T6, Fz, Cz, Pz, Oz, A1,A2, referenced to a common ground (GND). The data was sampled at 512 Hz. Figure S1 shows the EEG montage that was used during acquisition of the EEG data. Prior to EEG recordings being taken, certain basic preparations were carried out: cleaning the hair, adjustments of the EEG cap position, and impedance checking (was kept below 10 K ohm) were carried out in order to ensure good electrical contact with the scalp of the participants.

2.5. Experimental protocol

Participants were asked to sit on a comfortable chair, wearing the data glove on their right hand and their elbow resting on a flat surface table placed in front of them as shown in Fig. 1A. The acquisition session for each subject was of 16 min duration, consisting of a total of eight trials for each finger. The trials started with a 'RELAX' followed by 'WAIT', 'FINGER MOVEMENT', 'STOP' and 'END' visual cue, displayed on a laptop screen, indicating the subject to relax, wait, then perform finger movements, stop and end the session. Subjects were asked to focus on the screen while performing the displayed tasks. Fig. 1C depicts the timeline of the experimental protocol categorized into 5 stages as follows:

(0) S0 (Relax Stage): Screen displayed 'RELAX' cue and subject performed no movement for 25 s.

(1) S1 (Wait Stage): Screen displayed 'WAIT' cue and subject waited for 2 s to get ready before performing the movement.

(2) S2 (Movement Stage): Screen displayed 'FINGER MOVEMENT' along with a visual cue of a finger movement, and subject performed the movement for 12 s. The 'FINGER MOVEMENT' visual cue consisted of one of the following five movements: thumb flexion, index flexion, middle flexion, ring flexion and little flexion. All movements were performed in the above sequence during a trial in accordance with the visual cue being displayed.

(3) S3 (Stop Stage): Screen displayed 'STOP' cue indicating completion of the movement and subject stopped for 7 s. The subject performed S1 to S3 5 times during a trial, where at each time the subject performed a different finger movement according to the mentioned sequence.

(4) S4 (Rest stage): Screen displayed 'REST' cue indicating subject to rest for 10 s. This was done to reduce muscle fatigue in the subject before beginning the next trial. After S4, the subject performed S1 to S3 for the next trial. Overall, the subject performed S1 to S4 for a total of 8 times.

(5) S5 (End Stage): Screen displayed 'END' cue indicating the end of session, and subject performed no movement for 25 s.

2.6. Dataset

The dataset included 240 (6 subjects × 5 movements × 8 trials) 4-channel EMG, 240 (6 subjects × 5 movements × 8 trials) 22 - channel EEG movement trials, and 240 (6 subjects × 5 move-

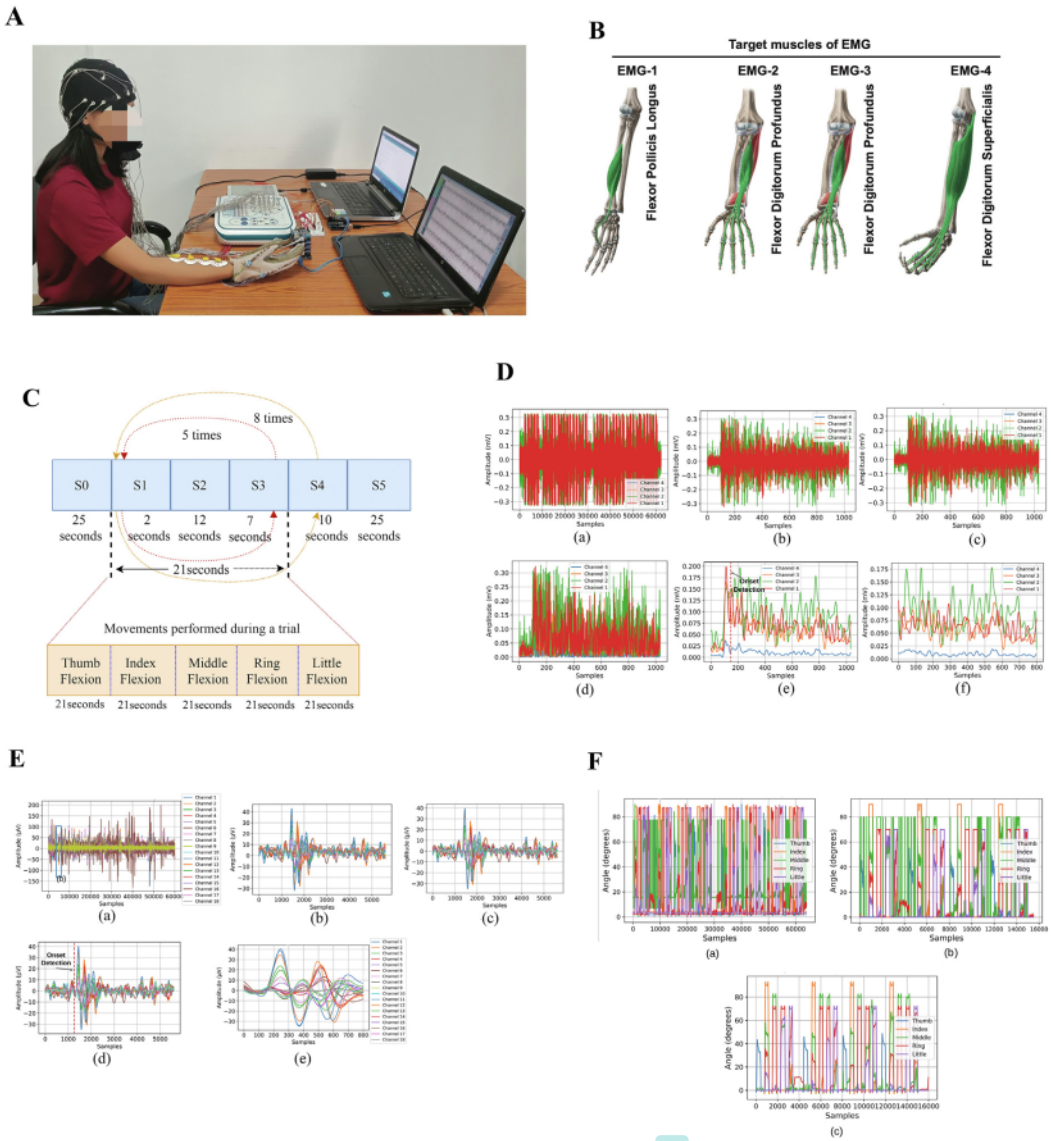

Fig. 1. **(A)** Experimental setup for EEG, EMG and finger kinematics data acquisition **(B)** Target muscle (flexor pollicis longus, flexor digitorum profundus, flexor digitorum superficialis) for placement of EMG electrodes **(C)** Timeline of experimental protocol **(D)** Pre-processing of EMG. (a) raw 4-channel EMG (b) enlarged view of a flexion trial and baseline correction (c) Filtering (d) Rectification (e) Onset detection (f) Segmentation of a flexion trial **(E)** Pre-processing of EEG. (a) raw 18-channel EEG (b) enlarged view of a flexion trial (c) baseline correction (d) filtering and Onset detection (e) and segmented EEG of a flexion trial **(F)** Pre-processing of finger kinematics (a) Raw MCP joint finger kinematics (b) Enlarged view of four trials (c) Filtering.

ments × 8 trials) finger kinematic data. Based on the data for subjects, the dataset was partitioned into 70 % for training and 30 % for testing, i.e., out of six subjects, data from four subjects were used for training and data from two subjects were used for testing.

2.7. Statistical analysis

A paired student's *t*-test was performed to compare the prediction and estimation performance of the implemented models. The t-tests were applied to results of the models used in estimating EMG from EEG and predicting finger movements and kinematics using estimated EMG. The level of significance was set at 5 % (alpha = 0.05).

3. Experimental results and discussion

3.1. EEG and EMG pre-processing

In this study, finger movements and kinematics were decoded in an online BCI scenario from EEG using AI algorithms. The dataset, comprised of EEG, EMG, and finger kinematics recordings was pre-processed in steps that included baseline correction, filtering, rectification, onset detection, and segmentation. A baseline correction algorithm was applied to raw EMG (Fig. 1D-a) to remove off-set from zero amplitude during no movement. The algorithm subtracted mean of the Rest stage samples corresponding to each channel from the Movement stage samples. To remove movement artefacts and

power line interference, the baseline corrected EMG (Fig. 1D-b) was filtered using a 6th order band pass Butterworth filter in the frequency range of 10–250 Hz, followed by a 50 Hz notch filter (Fig. 1-D-c) [24]. Following that, the filtered EMG was rectified, and a smooth envelope of the EMG was achieved using a low pass filter with a 4 Hz cut-off (Fig. 1D-d). The resulting EMG was then processed using a threshold detection algorithm for onset detection (Fig. 1D-e). Once the EMG amplitude exceeded a defined threshold level for more than fifty consecutive samples, the first sample was automatically marked as the movement onset point. After detection of the onset, the resulting EMG was segmented for further analysis using a non-overlapping window size of 250 ms (Fig. 1D-f). Similarly to EMG, EEG was pre-processed in steps that included baseline correction, filtering, onset detection, and segmentation. Raw EEG was baseline corrected (Fig. 1E-b, c) by subtracting mean of the Relax stage samples across 22 EEG channels from the Movement stage raw EEG samples. For final analysis, 18 channels of EEG for was selected for the proposed study (Fig. 1E-a). To remove movement artefacts and power line interference, the corrected EEG was filtered using a 2nd order band pass Butterworth filter within a frequency range of 0.1–40 Hz and a 50 Hz notch [25]. This was followed by detection of onset of movement in EEG (Fig. 1E-d). Using a non-overlapping window of 250 ms, the resulting EEG was finally segmented for further analysis (Fig. 1E-e). Next, the finger kinematics data was pre-processed with a low pass filter (cut-off frequency = 10 Hz) (Fig. 1F-a,e) and segmented to a window size of 250 ms for each movement (Figure S3).

3.2. Finger movement and finger kinematics prediction framework

Predicting each finger movement in coordination using EEG signal necessitates complex processing algorithms that must be applied in stages [6,26]. Since, each stage employs a different algorithm for sequential training, it makes the overall adaptive system complex. To this end, deep learning methods aid in the simultaneous processing of multiple signals to achieve high performance with satisfactory accuracy in real-time. It offers a single learning algorithm for training several signals in parallel to increase decoding performance [27]. The proposed study, uses a deep neural network comprising of a LSTM network for predicting finger movements and an ensemble learning method comprising of a random forest regressor was used for estimating the finger kinematics.

Fig. 2A depicts the framework used to predict finger movements and kinematics through EMG estimation EMG from EEG. This framework was accomplished in three stages. The first stage involved predicting the type of finger movement using acquired EMG after it had been pre-processed. As described in section 2.6, the dataset was used accordingly for training and testing. Using the acquired EMG, a LSTM network model was trained for prediction of five finger movements of the right hand: thumb flexion, index flexion, middle flexion, ring flexion and little flexion. The model's performance was validated using 5-fold cross validation. For a comparative analysis of the prediction model, a Convolutional Neural Network-Long Short-Term Memory (CNN-LSTM) network, a Convolutional LSTM (Conv-LSTM) network, and a random forest model were also evaluated. The second stage involved predicting the type of finger movement using estimated EMG. Following pre-processing, the EEG was used to train a linear regression model to estimate the 4-channel EMG from the corresponding 18-channel EEG. A 5-fold cross validation was also used to validate the linear regression model. This was followed by the prediction of finger movements with estimated EMG using the trained prediction model obtained in the first stage. The third stage involved predicting the finger kinematics from acquired EMG and estimated EMG. Following pre-processing, the finger kinematics were used to train a random forest regression model to predict the joint angle kinematics of five fingers: thumb MCP, index MCP, middle MCP, ring MCP and little MCP from the corresponding acquired EMG. 5-fold cross validation was used to validate the model. A linear regression, k-nearest neighbours (KNN), ridge, and LSTM models were also evaluated for a comparative analysis. The prediction of finger kinematics with estimated EMG was then followed using the trained prediction model obtained earlier in this stage.

3.3. Prediction models

3.3.1. Prediction model for finger movements prediction

Deep learning (DL) neural networks manages to deliver high accuracy without the need to input hand-extracted features into the network for training. A LSTM network is one such DL network that performs automatic feature extraction from time-series data and captures the temporal information, delivering a high accuracy [28,29]. In presented study, a LSTM network was implemented for the prediction of finger movements from EMG. The LSTM network learned better by remembering the sequential information of the input EMG samples in short time steps. The LSTM unit is comprised of a forget gate layer, input gate layer, output gate layer and state gate layer. The forward pass equations of a LSTM unit with a forget gate layer are described from Equation (1) to Equation (6).

$$i_t = \sigma(W_i * [h_{t-1}, x_t] + b_i) \quad (1)$$

$$f_t = \sigma(W_f * [h_{t-1}, x_t] + b_f) \quad (2)$$

$$o_t = \sigma(W_o * [h_{t-1}, x_t] + b_o) \quad (3)$$

$$\tilde{c} = tanh(W_c * [h_{t-1}, x_t] + b_t) \quad (4)$$

$$c_t = f_t * c_{t-1} + i_t * \tilde{c}_t \quad (5)$$

$$h_t = o_t * tanh(c_t) \quad (6)$$

where t, i, o, f and c denote the time steps, input gate, output gate, forget gate, and cell state respectively. W_i, W_f, W_o,W_c denotes the input gate, forget gate, output gate, and cell state weights respectively and b denotes the unit's bias. These equations suggested that the activation value of a LSTM unit required knowledge of the previous value in time. The input gate i_t and forget gate f_t, controlled how much of the previous hidden state h_{t-1} and current input x_t was contributed to the cell state c_t. The sigmoid function σ scaled the activation of the forget, input, and output gates, and to finally get the prediction result from the model the hidden state was filtered with the hyperbolic tangent function *tanh*.

The LSTM model developed for this study was a four-layered architecture (Fig. 2B). The input layer had 150 nodes, followed by two hidden layers: a recurrent layer with 200 LSTM cells and a fully - connected dense layer of 250 units. At the last, was a dense output layer with 5 units for five movements. The activation function used in the hidden and output layer was a rectifier (reLU) and softmax function respectively. Softmax function in the output layer gave a probability distribution for the prediction output. To avoid model over-fitting, a dropout regularization of 20 percent was applied to the input and hidden layers and was trained with the early stopping method. A manual search was used to determine the network's parameters based on the input parameter value that provided highest accuracy. The network had 425,556 parameters that were optimized using the ADAM version of stochastic gradient descent (SGD), with a learning rate of 0.001, a sparse categorical loss function, and a batch size equal to sequence length of the input EMG samples (800-time steps). The sparse categorical loss was chosen in the LSTM model to address the multi-class prediction problem with integer target values so that the model labels the

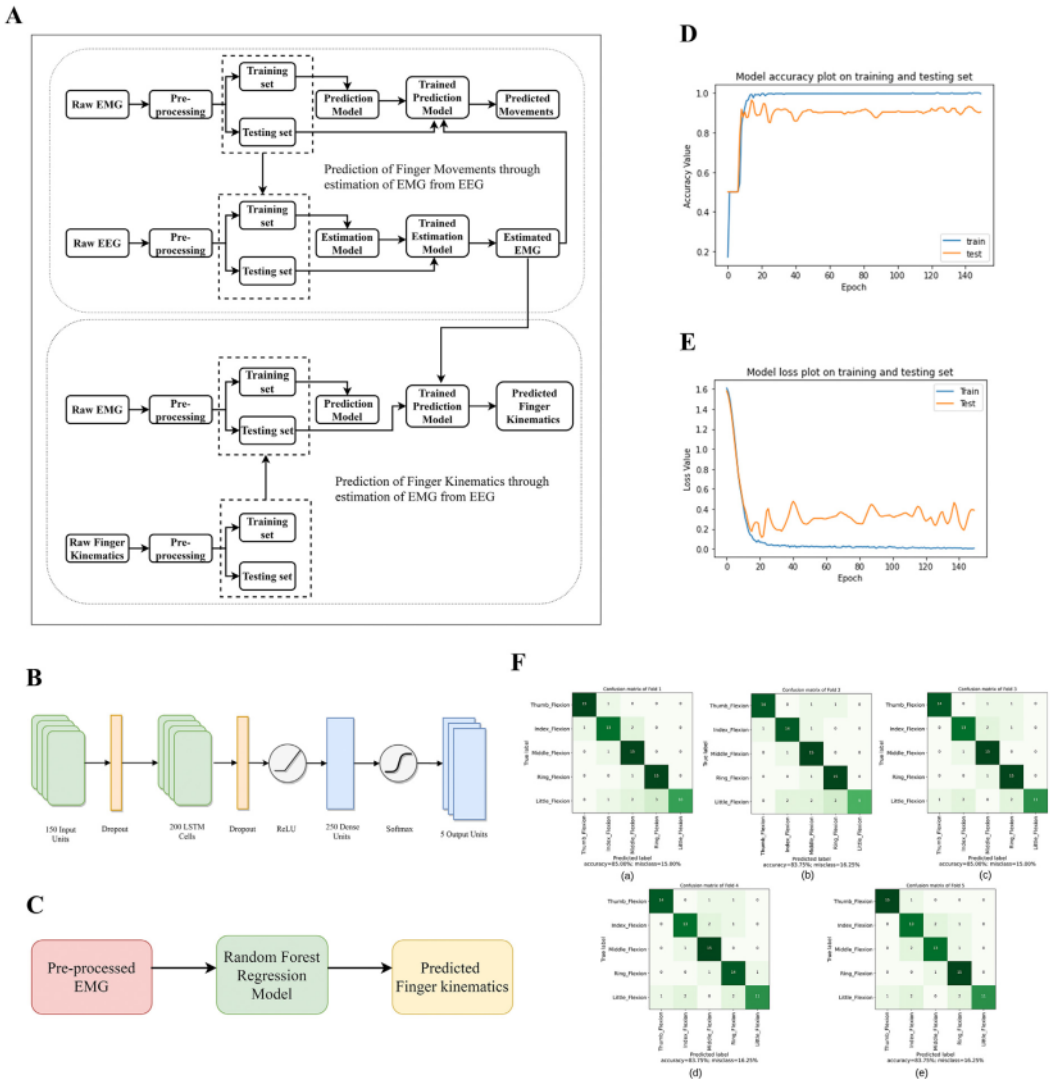

Fig. 2. **(A)** Framework for prediction of finger movements and finger kinematics through estimation of EMG from EEG **(B)** Configuration of implemented LSTM model **(C)** Configuration of implemented random forest regression model **(D)** LSTM model's accuracy plot on training and testing set across 150 epochs depicting the prediction accuracy during training and testing (E) LSTM model's loss curve on training and testing set across 150 epochs **(F)** Confusion matrix obtained during (a) fold 1 (b) fold 2 (c) fold 3 (d) fold 4 (e) fold 5 using acquired EMG.

predicted type of finger movement as integer values rather than one-hot encoded labels. Also, it had the benefit of requiring less memory and computation time. For n number of prediction classes, Equation (7) described the sparse categorical loss function (SCF).

$$SCF = -\sum_{i=1}^{n} t_i \log(p_i) \quad (7)$$

where t_i is the target label and p_i is the softmax probability for the i^{th} class.

3.3.2. Prediction model for finger kinematics prediction

Random forest is an ensemble learning algorithm that uses decision trees to solve classification and regression problems. A random forest regression model predicts the target data more accurately by averaging the output of multiple decision trees in the ensemble. In comparison to other regression models for predicting hand kinematics, a random forest regression model is simpler to train and resistant to outliers and noise. Its processing time during training is faster than that of a neural network because it can be parallelized. It can also process time series data with automatic feature extraction [30]. In this study, a random forest regression model was used to predict finger kinematics from EMG data (Fig. 2C). The model's input was pre-processed EMG, and output was the predicted MCP joint angles. The parameters of random forest model consisted of 15 number of trees in the forest and value 5 as the maximum depth of the trees. These parameters were determined by a manual search based on the value of the input parameter that gave the lowest error.

3.4. Estimation model

The proposed study employs a novel method for fusing EEG and EMG. A regression technique based on linear regression is used to

estimate 4-channel EMG from 18-channel EEG, corresponding to five types of finger movements. The regression model was applied to establish a linear pathway between EEG and EMG in order to estimate EMG from EEG since the regression algorithm is based on the assumption that the independent variable is related to the dependent variable [31]. In this estimation model, the independent variable was EEG, which was input, and dependent variable was EMG to be estimated. The linear regression model implemented is described by Equation (8).

$$Yi = \beta i_0 + \beta i_1 * Xi_1 + \epsilon \tag{8}$$

where i = 1,2,3,4,….n (n = number of samples), Xi_1 is i^{th} 18-channel input EEG sample and Yi was i^{th} 4-channel EMG to be estimated by the model. Estimation coefficients of the model were given by values of βi_0 i.e., regression EEG intercept, βi_1 i.e., regression coefficient and ϵ was the error in the model.

3.5. Prediction of finger movements and kinematics from EEG through estimation of EMG

Results obtained for prediction of finger movements and kinematics from EEG via estimation of EMG involving various stages, as well as the performance of the models in terms of their evaluation metrics and comparison analysis with other models, are presented in this section. The hardware used for performing all the experiments in the study was on a Intel i7-5500U CPU 64-bit 2.40 GHz processor with 8.00 GB RAM memory.

3.5.1. Prediction of finger movements using acquired EMG

The finger movement prediction model was trained for 150 epochs applying early stopping method using acquired EMG. Fig. 2-D-E shows the learning curves for average prediction accuracy and loss of the LSTM model during training and testing across 150 epochs indicating that as the loss decreased with number of epochs, the accuracy increased, resulting in an optimal result at the end of 150 epochs. 5-fold cross validation evaluated the model's performance and gave the best prediction model. The model's accuracy was reported in average accuracy over 5-fold cross validation results and across six subjects. The prediction accuracy obtained for each fold across five movements was evaluated using Equation (9).

$$A_i = \sum_1^5 i \frac{TPi + TNi}{TPi + TNi + FPi + FNi} \tag{9}$$

where i is the number of movements across which average accuracy was evaluated. TP, TN, FP and FN are true positive, true negative, false positive and false negative predictions respectively [32].

Confusion matrices were obtained representing the number of correctly predicted movements i.e., the true positives and number of incorrectly predicted movements i.e., the true negatives during testing for each fold. The diagonal of the confusion matrices highlighted the correctly predicted movements (Figure S4; Supplementary Material). Average prediction accuracy of the LSTM model for each movement across all test subjects showed a maximum of (97.50 ± 5.00) % for thumb and middle finger while for index and ring finger it was above 93.75 %. Lowest average prediction accuracy of 88.75 % was obtained by little finger (Fig. 3A). This was indicative of the model being able to predict thumb and middle flexion predominantly followed by prediction of index and ring finger flexions, while finding most difficulty in predicting little finger flexion. A reason for this could be due to the accurately performed thumb and middle finger movements by the subjects during the experiment. The average prediction accuracy achieved across five movements and all test subjects was (94.75 ± 0.93)% with each fold obtaining a prediction accuracy above 93.75 % (Fig. 3B), indicating a good performance of the prediction model in predicting the movements using the acquired EMG.

In a comparative analysis, when the LSTM model was compared with other models such as CNN-LSTM, ConvLSTM, and random forest, the LSTM model's average prediction accuracy demonstrated an average 0.21 % higher accuracy than CNN-LSTM and ConvLSTM models and a 12.45 % higher accuracy than random forest model (Fig. 3C). However, the processing time (i. e., time taken by the model during training) was higher in LSTM model as compared to CNN-LSTM and ConvLSTM (Fig. 3D). This was because CNN-LSTM and ConvLSTM models attained a faster state of convergence during their model training in fewer epochs than LSTM model. In the presented experiment, CNN-LSTM and ConvLSTM took 65 and 70 epochs respectively. Whereas it consumed more epochs for the LSTM network to attain that convergence state, which was 150 in our experiment. Although the training time per epoch for CNN-LSTM (i.e., 13.00 s) and ConvLSTM (i.e.,12.00 s) were longer compared to LSTM (i.e., 11.60 s) due to the complexity of their convolution layers, the aggregated training time over a number of epochs for CNN-LSTM and ConvLSTM were less i.e., 900 s and 906 s compared to 2500 s for LSTM. This is also substantiated by the fact that the special structure of CNN and Convolution can reduce the complexity as well as the overall training time of the model [33] and can remember much longer sequences compared to LSTM [34]. The LSTM model was chosen for prediction of finger movements due to its higher accuracy, although it had a longer computation time.

3.5.2. Prediction of finger kinematics using acquired EMG

Performance of the prediction model implemented for prediction of finger kinematics using acquired EMG, was evaluated by two metrics: root mean squared error (RMSE), and coefficient of determination (R^2). RMSE measured the square root of the difference between predicted and target values using Equation (10).

$$RMSE = \sqrt{\sum_{i=1}^{N} \frac{(y_i - x_i)^2}{N}} \tag{10}$$

where y_i is the target value of sample i, x_i is the i^{th} predicted value and N is the total number of samples taken for evaluation. R^2 gave the difference between predicted and target values in terms of their amplitude and correlation. It was calculated using Equation (11).

$$R^2 = 1 - \frac{\sum_{i=1}^{N} (y_i - x_i)^2}{\sum_{i=1}^{N} (y_i - \bar{x}_i)^2} \tag{11}$$

where y_i is the target value of sample i, x_i is the predicted value of sample i, and $\bar{x}_i$ is the mean of y_i. R^2 of a good prediction is between 0 and 1 and for a perfect prediction it is close to 1.

A random forest regression model was trained for the prediction of finger kinematics. An average RMSE (Fig. 3E) of (0.258 ± 0.017) degree and an average R^2 (Fig. 3F) of 0.842 ± 0.015 was achieved over 5-fold cross validation across five fingers' MCP joint angles and all subjects. This result indicated a low error in predicting the finger kinematics using acquired EMG, and a good model prediction using acquired EMG across five fingers' joint angles and all subjects. The thumb and ring finger MCP joint angle showed an average RMSE error of (0.24 ± 0.015) and (0.27 ± 0.016) respectively followed by the middle finger joint angle which showed an average RMSE error of 0.28 ± 0.014 (Fig. 3G). The index and little finger MCP joint angle showed a comparatively higher error than the rest of the finger joint angles. It may be understood that while the model predicted the thumb, middle and ring MCP joint angles very well, it poorly predicted the little finger MCP joint angle. The reason for this could be that while performing flexion of little finger, other fingers got flexed along, thereby making the model difficult to correctly distinguish it

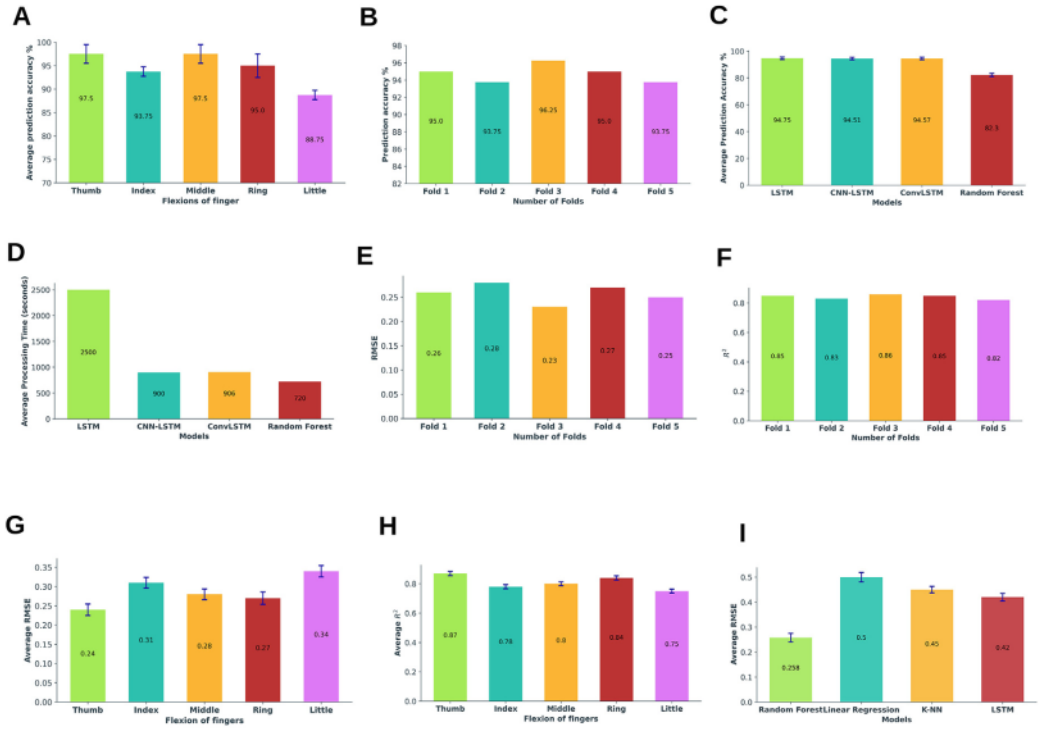

Fig. 3. **(A)** Average prediction accuracy of LSTM model for each finger movement across six subjects and five folds using acquired EMG **(B)** Prediction accuracy of LSTM model across five movements and at each fold using acquired EMG **(C)** Comparison of LSTM, CNN-LSTM and ConvLSTM models in terms of average prediction accuracy using acquired EMG **(D)** Comparison of LSTM, CNN-LSTM and ConvLSTM models in terms of average processing time across five movements and six subjects using acquired EMG **(E)** Prediction performance of random forest regression model in terms of RMSE across finger kinematics of five fingers and six subjects at each fold using acquired EMG **(F)** Prediction performance of random forest regression model in terms of R^2 across finger kinematics of five fingers at each fold using acquired EMG **(G)** Prediction performance of random forest regression model in terms of average RMSE for each finger MCP joint angle across six subjects and 5-folds **(H)** Prediction performance of random forest regression model in terms of average R^2 for each finger MCP joint angle across six subjects and 5-folds **(I)** Comparison results of random forest regression with linear regression, and K-NN regression model on the basis of their average RMSE.

from the joint angles of other fingers. Comparison between the performance of random forest regression model with KNN regression, linear regression and a LSTM regression models depicted in Fig. 3I, showed random forest outperforming the aforementioned models based on RMSE and R^2 metrics (Table S2; Supplementary Materials). Random forest model gave an average of around 0.22 degree lesser error than the other models and showed a high correlation of 0.84 demonstrating a strong linear relationship between the acquired EMG and finger kinematics.

3.5.3. Estimation of EMG from EEG

4-channel EMG for finger movements: thumb, index, middle, ring and little finger flexion were estimated from corresponding 18-channel EEG using linear regression. The average 5-fold cross validation result evaluated in terms of RMSE and R^2 using the linear regression model across five movements and all subjects (Table S3) was 0.55 ± 0.014 and 0.74 ± 0.007 respectively. This showed good estimation of the EMG from EEG with a low error. 18 channels of EEG from a total 22 EEG channels was selected for EMG estimation based on the linear regression model's performance during estimation and prediction of the movements by LSTM model with the estimated EMG. The process provided optimal number of channels to be used for obtaining estimation and prediction performance result (Table S4). In a comparative analysis, the linear regression model produced an average of around 0.0086 degree lesser error and higher correlation (0.742) than that of random forest, KNN and ridge estimation models in terms of average RMSE, average R^2, and average processing time. This indicated a good estimation of EMG from EEG and depicted that EEG has a somewhat linear relationship with the estimated EMG (Table S5).

3.5.4. Prediction of finger movements using estimated EMG

Estimated EMG obtained using linear regression model was tested with the trained LSTM model for prediction of desired finger movement. The average prediction accuracy of LSTM model for each finger movement across all subjects and five folds using estimated EMG showed highest prediction accuracy in ring finger (92.50 ± 2.5)%, followed by middle, thumb, and index finger (Fig. 4A). The index finger displayed the lowest prediction accuracy (65 %) using estimated EMG. Like in prediction using acquired EMG, these results showed the model's ability to easily predict thumb, ring middle and index finger flexions but difficulty in predicting little finger flexion. The confusion matrices results during 5-fold cross validation (Fig. 2F) showed more than a 83 % accuracy at each fold and the average accuracy was (84.25 ± 0.61)% across five movements and all subjects (Fig. 4B). These are further indicative of a good model performance using estimated EMG at power with the performance achieved using acquired EMG. Thus, suggesting that the proposed hierarchical approach can satisfactorily predict finger movements using estimated EMG. Moreover, comparison with CNN-LSTM, ConvLSTM, and random forest classifier models using estimated EMG, the LSTM model showed around 0.5 % higher average prediction accuracy than those models (Fig. 4C). Statistical analysis evaluated with a paired *t*-test revealed LSTM model per-

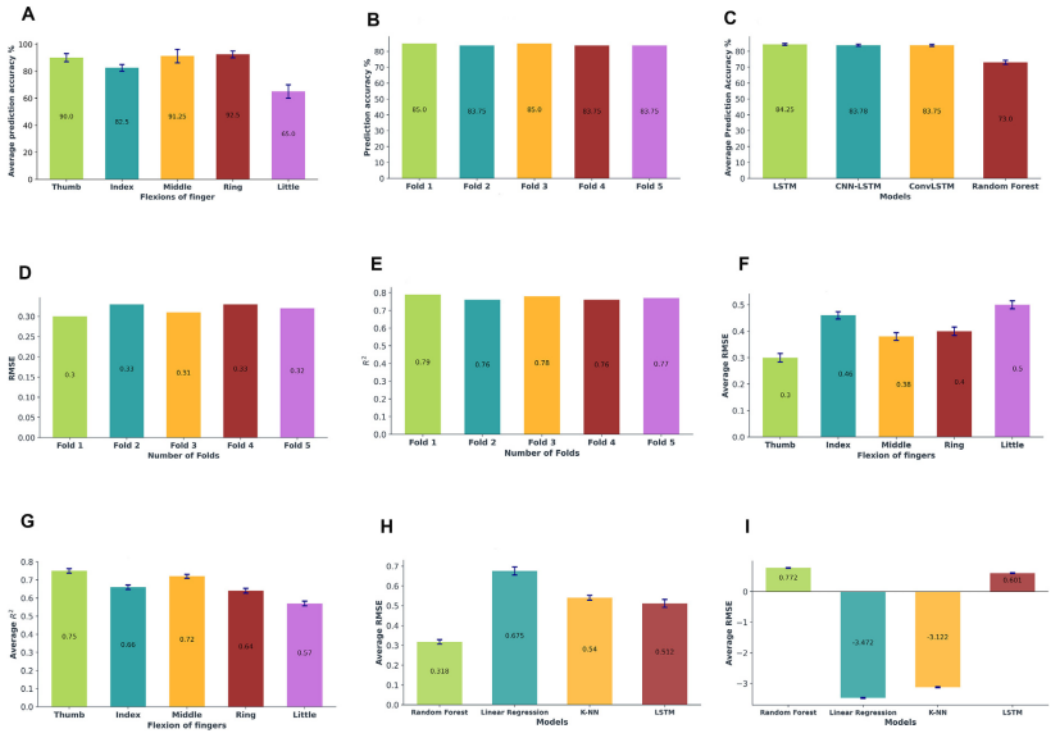

Fig. 4. **(A)** Average prediction accuracy of LSTM model for each finger movement across six subjects and five folds using estimated EMG **(B)** Prediction accuracy of LSTM model across five movements and six subjects at each fold using estimated EMG **(C)** Comparison of average prediction accuracy between LSTM, CNN-LSTM and ConvLSTM model across five movements and six subjects using estimated EMG **(D)** Prediction performance of random forest regression model in terms of average RMSE across finger kinematics of five fingers and six subjects at each fold using acquired EMG **(E)** Prediction performance of random forest regression model in terms of R^2 across finger kinematics of five fingers at each fold using estimated EMG **(F)** Prediction performance of random forest regression model in terms of average RMSE for each finger MCP joint angle across six subjects and 5-folds using estimated EMG **(G)** Prediction performance of random forest regression model in terms of average R^2 for each finger MCP joint angle across six subjects and 5-folds using estimated EMG **(H)** Comparison between random forest regression, linear regression, KNN regression and LSTM model in terms of average RMSE **(I)** Comparison between random forest regression, linear regression, KNN regression and LSTM model in terms of average R^2.

forming better than the aforementioned prediction models having a p-value < 0.05 (Table S8). These observations together with the comparison shown between the models in terms of accuracy and processing time in Fig. 3C and Fig. 3D led to selection of the LSTM model for the proposed study in prediction of finger movements.

3.5.5. Prediction of finger kinematics using estimated EMG

Using the trained random forest regression model, the finger kinematics were predicted from estimated EMG. An average RMSE of (0.318 ± 0.011) (Fig. 4D) and average R^2 of (0.772 ± 0.011) (Fig. 4E) over 5-fold cross-validation across five fingers and all subjects was achieved for the random forest regression model using estimated EMG. This demonstrated a good performance of the regression model having a low error and satisfactory estimation of finger joint angles using the estimated EMG. The thumb and middle MCP joint angle's average error in terms of RMSE was (0.30 ± 0.016) and (0.38 ± 0.014) (Fig. 4F) while the average R^2 was 0.75 and 0.72 respectively (Fig. 4G). The highest error was reported in little finger joint angle (RMSE = 0.50 ± 0.015) and index finger joint angle (RMSE = 0.46 ± 0.014) prediction. An average of around 0.1 degree higher error and around 0.13 lower average R^2 value in predicting thumb, middle, and ring finger joint angles using estimated EMG was revealed than in their prediction using acquired EMG. This suggested that the model performed well for thumb, middle, ring and to a some extent for index finger but performed poorly for the little finger joint angle. The prediction of finger kinematics using acquired EMG gave a better result than prediction using estimated EMG since in the former case the prediction was achieved using pre-processed EMG which was obtained from the direct source of its generation thereby yielding a much lesser error than using estimated EMG. On comparing the random forest regression model with linear regression, KNN regression, and a LSTM model in terms of RMSE and R^2 (Fig. 4H-I), the random forest regression model showed an average of around 0.26 degree lesser error and a 2.77 higher R^2 value than the other models. The paired student *t*-test results (Table S8) too showed that the random forest ($p < .05$) had a statistically significant difference in performance than those models. Between LSTM and random forest model, the random forest model performed better as depicted in Fig. 4H-I (Table S2, Table S8) and thus selected for our proposed study. The paired *t*-test statistical analysis between LSTM and random forest further justified use of the specific models in predicting finger movements and estimating finger kinematics respectively.

3.6. Emulation of estimated finger movements and kinematics in a prosthetic hand

Results of estimated finger movements and kinematics were emulated into a prosthetic hand finger movement control. A five fingered prosthetic hand prototype was customized with angle sensors at MCP joints. Estimation of finger kinematics was

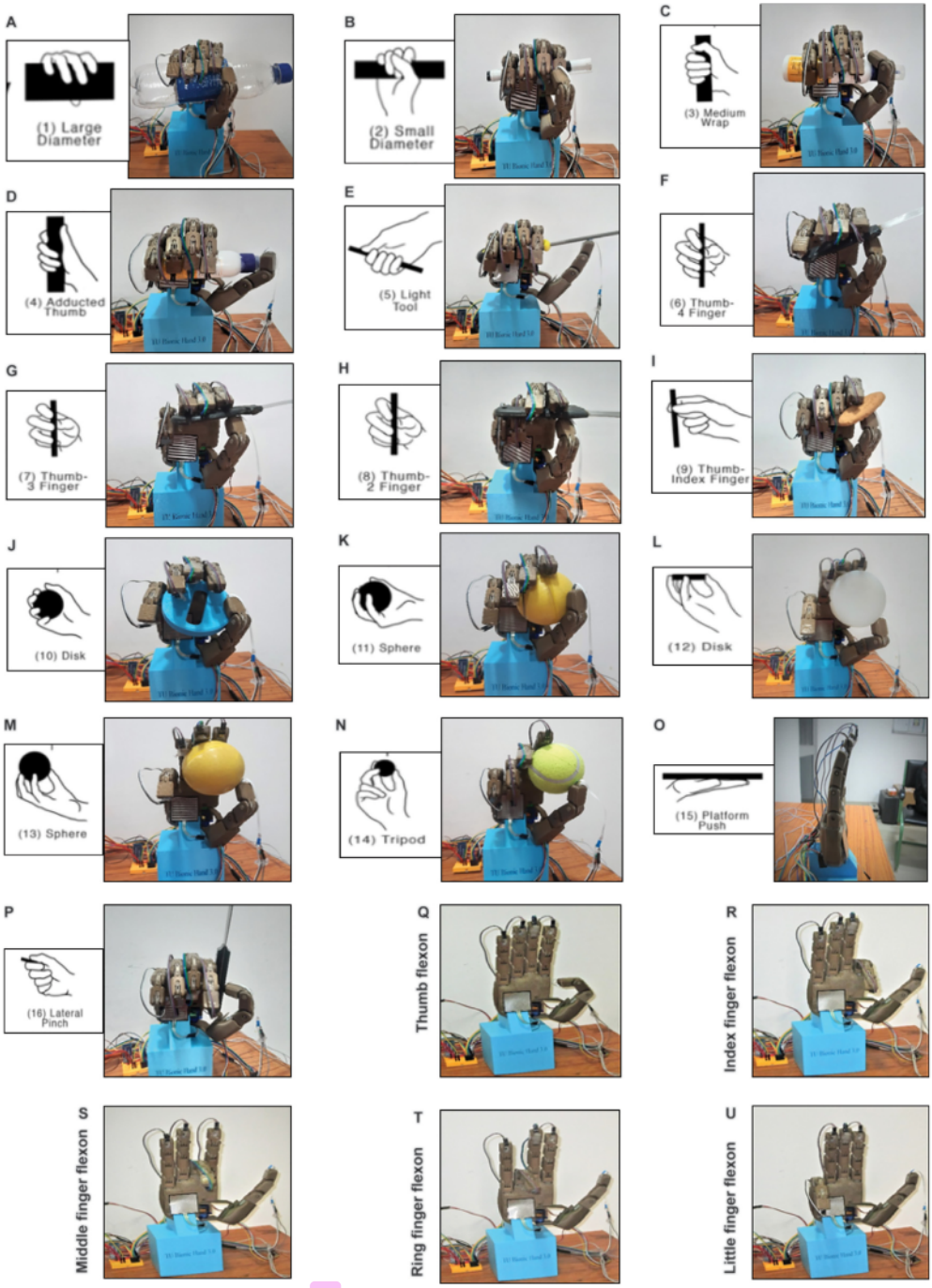

Fig. 5. 16-Grasp types following Cutkosky's grasp taxonomy and five finger movements by the prosthetic hand using the reported EEG-EMG based finger movement and kinematics estimation.

employed as superior control for commanding a proportional derivative controller to emulate the estimated results into the hand. Following the hierarchical approach for fusion of EEG and EMG for predicting finger movements and kinematics, the model has been tested for detection of simultaneous finger movements and kinematics. Thereby, the prosthetic hand could perform 16-grasp types of Cutkosky's grasp taxonomy and individual finger movements as presented in Fig. 5.

4. Conclusion

Presented work successfully demonstrated prediction of finger movements, finger kinematics through EMG estimation from EEG using machine learning techniques integrated with BCI-AI networking. The final result presented prediction of finger kinematics from the EEG with estimation of EMG from EEG as an intermediate step as presented in section 3.5.3 to 3.5.5. In addition, the finger movements were also predicted from EEG with intermediate steps of estimating EMG. These results have been used for emulating the identified finger movement and kinematics into a prosthetic hand prototype as presented in section 3.6. The research has emphasized the significance of EEG and EMG fusion, utilizing the process of estimating EMG from EEG in development of hybrid BCI-AI systems, which has not been reported in literature to the best of the authors' knowledge. AI integration with BCI systems has empowered the designed hierarchical approach in attaining the high accuracy prediction of finger movements and finger kinematics. Synchronisation of EEG and EMG provide an efficient prediction of finger movements due to high coherence index co-linearity. Although BCI systems have earned their recognition, the state-of-art BCI integration with AI networking has a broad spectrum to explore for ideal interpretation of brain's normal output pathways of peripheral nerves and muscles. The work presented is highly recommended for implementation in the development of robotic limb prosthesis and rehabilitation for amputees to ease the recognition and prediction of limb movements at clinical settings. Furthermore, it has been established that the proposed hierarchical method can estimate finger kinematics and finger movements based on the fusion of EEG and EMG for control of real-time prototype and can be extended to 3D applications. Another prospect of the presented work is to extend for multi-objective optimization using 3D point clouds and 3D mesh to provide for cost-effective, flexible and scalable solutions.

5. Data and materials availability

All the data are available in the main text or supplementary materials. Code of this study is openly available at http://www.tezu.ernet.in/erl/sm.html.

CRediT authorship contribution statement

Tanaya Das: Conceptualization, Data Curation, Formal analysis, Methodology, Investigation, Software, Visualization, Writing-original draft, Writing-review & editing. **Lakhyajit Gohain:** Hardware Design, Writing-review & editing. **Nayan M Kakoty:** Conceptualization, Funding Acquisition, Project Administration, Resources, Supervision, Methodology, Writing-review & editing, Hardware design. **MB Malarvili:** Conceptualization, Funding acquisition, Writing-review & editing. **Prihartini Widiyanti:** Conceptualization, Funding acquisition, Writing-review & editing. **Gajendra Kumar:** Conceptualization, Funding acquisition, Writing-original draft, Writing-review & editing.

Data availability

Datasets generated during this study are available from the corresponding author on resonable request.

Declaration of Competing Interest

The authors declare that they have no known competing financial interests or personal relationships that could have appeared to influence the work reported in this paper.

Acknowledgements

The support received in the project number CRD/2018/000049 under the department of Science and Technology (DST), Government of India; project number NECBH/2019-20/144 under the department of Biotechnology, Government of India; project number GP/2021/RR/018 under the I-Hub Foundation for Cobotics-Indian Institute of Technology Delhi, DST, Government of India and The Health and Medical Research Fund (HMRF) under Food and Health Bureau, Hong Kong Special Administrative Region Government (08193956) are gratefully acknowledged.

Appendix A. Supplementary data

Supplementary data to this article can be found online at https://doi.org/10.1016/j.neucom.2023.01.061.

References

[1] C.L. McDonald, S. Westcott-McCoy, M.R. Weaver, J. Haagsma, D. Kartin, Global prevalence of traumatic non-fatal limb amputation, Prosthet. Orthot. Int. 45 (2) (2021) 105–114, https://doi.org/10.1177/0309364620972258.
[2] J. Lobo-Prat, P.N. Kooren, A.H. Stienen, J.L. Herder, B.F. Koopman, P.H. Veltink, Non-invasive control interfaces for intention detection in active movement-assistive devices, J. Neuroeng. Rehabil. 11 (2014) 168, https://doi.org/10.1186/1743-0003-11-168.
[3] A.I. Sburlea, L. Montesano, R. Cano de la Cuerda, I.M. Alguacil Diego, J.C. Miangolarra-Page, J. Minguez, Detecting intention to walk in stroke patients from pre-movement EEG correlates, J. Neuroeng. Rehabil. 12 (2015) 113, https://doi.org/10.1186/s12984-015-0087-4.
[4] A. Toda, H. Imamizu, M. Kawato, M.A. Sato, Reconstruction of two-dimensional movement trajectories from selected magnetoencephalography cortical currents by combined sparse Bayesian methods, Neuroimage 54 (2) (2011) 892–905, https://doi.org/10.1016/j.neuroimage.2010.09.057.
[5] F. Artoni, E. Pirondini, A. Panarese, S. Micera, Exploring neuro-muscular synergies of reaching movements with unified independent component analysis, Annu. Int. Conf. IEEE Eng. Med. Biol. Soc. 2016 (2016) 3183–3186, https://doi.org/10.1109/EMBC.2016.7591405.
[6] N. Yoshimura, H. Tsuda, T. Kawase, H. Kambara, Y. Koike, Decoding finger movement in humans using synergy of EEG cortical current signals, Sci. Rep. 7 (1) (2017) 11382, https://doi.org/10.1038/s41598-017-09770-5.
[7] M. Barsotti, S. Dupan, I. Vujaklija, S. Dosen, A. Frisoli, D. Farina, "Online Finger Control Using High-Density EMG and Minimal Training Data for Robotic Applications," (in English), IEEE Robot Autom Let 4 (2) (2019) 217–223, https://doi.org/10.1109/Lra.2018.2885753.
[8] J. H. Cho, J. H. Jeong, D. J. Kim, and S. W. Lee, "A Novel Approach to Classify Natural Grasp Actions by Estimating Muscle Activity Patterns from EEG Signals," (in English), I Wint C Brain-Comp, pp. 24-27, 2020. [Online]. Available: <Go to ISI>://WOS:000612527100008.
[9] D. Camargo-Vargas, M. Callejas-Cuervo, S. Mazzoleni, Brain-Computer Interfaces Systems for Upper and Lower Limb Rehabilitation: A Systematic Review, Sensors (Basel) 21 (13) (2021), https://doi.org/10.3390/s21134312.
[10] X. Zhang et al., The combination of brain-computer interfaces and artificial intelligence: applications and challenges, Ann. Transl. Med. 8 (11) (2020) 712, https://doi.org/10.21037/atm.2019.11.109.
[11] S. Olsen, J. Zhang, K.F. Liang, M. Lam, U. Riaz, J.C. Kao, An artificial intelligence that increases simulated brain-computer interface performance, J. Neural Eng. 18 (4) (2021), https://doi.org/10.1088/1741-2552/abfaaa.
[12] I. Tobore et al., Deep Learning Intervention for Health Care Challenges: Some Biomedical Domain Considerations, JMIR Mhealth Uhealth 7 (8) (2019) e11966.
[13] A.R. Asif et al., Performance Evaluation of Convolutional Neural Network for Hand Gesture Recognition Using EMG, Sensors (Basel) 20 (6) (2020), https://doi.org/10.3390/s20061642.
[14] A. Muralidharan, J. Chae, D.M. Taylor, Early detection of hand movements from electroencephalograms for stroke therapy applications, J. Neural Eng. 8 (4) (2011), https://doi.org/10.1088/1741-2560/8/4/046003.
[15] N.A. Bhagat et al., Neural activity modulations and motor recovery following brain-exoskeleton interface mediated stroke rehabilitation, Neuroimage Clin. 28 (2020), https://doi.org/10.1016/j.nicl.2020.102502.
[16] P.D.E. Baniqued et al., Brain-computer interface robotics for hand rehabilitation after stroke: a systematic review, J. Neuroeng. Rehabil. 18 (1) (2021) 15, https://doi.org/10.1186/s12984-021-00820-8.
[17] A. Schwarz, M.K. Holler, J. Pereira, P. Ofner, G.R. Muller-Putz, Decoding hand movements from human EEG to control a robotic arm in a simulation environment, J. Neural Eng. 17 (3) (2020), https://doi.org/10.1088/1741-2552/ab882e.
[18] M.A. Bockbrader, G. Francisco, R. Lee, J. Olson, R. Solinsky, M.L. Boninger, Brain Computer Interfaces in Rehabilitation Medicine, PM R 10 (9 Suppl 2) (2018) S233–S243, https://doi.org/10.1016/j.pmrj.2018.05.028.

[19] W. Tang, F. He, Y. Liu, YDTR: Infrared and Visible Image Fusion via Y-shape Dynamic Transformer, IEEE Trans. Multimedia (2022), https://doi.org/10.1109/TMM.2022.3192661.
[20] W. Tang, F. He, Y. Liu, Y. Duan, MATR: Multimodal Medical Image Fusion via Multiscale Adaptive Transformer, Trans. Img. Proc. 31 (2022) 5134–5149, https://doi.org/10.1109/TIP.2022.3193288.
[21] H. Leon-Garza, H. Hagras, A. Peña-Rios, A. Conway, G. Owusu, A type-2 fuzzy system-based approach for image data fusion to create building information models, Inf. Fusion 88 (2022) 115–125, https://doi.org/10.1016/j.inffus.2022.07.007.
[22] World Medical Association. "World Medical Association Declaration of Helsinki: Ethical Principles for Medical Research Involving Human Subjects," JAMA, 310(20), pp. 2191–2194,2013, doi:10.1001/jama.2013.281053.
[23] G. Pfurtscheller, C. Neuper, and G. Krausz, "Functional dissociation of lower and upper frequency mu rhythms in relation to voluntary limb movement", Clinical Neurophysiology 111, 1873–1879.
[24] H.G. Kortier, V.I. Sluiter, D. Roetenberg, P.H. Veltink, Assessment of hand kinematics using inertial and magnetic sensors, J. Neuroeng. Rehabil. 11 (2014) 70, https://doi.org/10.1186/1743-0003-11-70.
[25] J.R. Potvin, S.H. Brown, Less is more: high pass filtering, to remove up to 99% of the surface EMG signal power, improves EMG-based biceps brachii muscle force estimates, J. Electromyogr. Kinesiol. 14 (3) (2004) 389–399, https://doi.org/10.1016/j.jelekin.2003.10.005.
[26] R.U. Alam, H. Zhao, A. Goodwin, O. Kavehei, A. McEwan, Differences in Power Spectral Densities and Phase Quantities Due to Processing of EEG Signals, Sensors (Basel) 20 (21) (2020), https://doi.org/10.3390/s20216285.
[27] K. Kritsis, M. Kaliakatsos-Papakostas, V. Katsouros, and A. Pikrakis, "Deep Convolutional and LSTM Neural Network Architectures on Leap Motion Hand Tracking Data Sequences," (in English), Eur Signal Pr Conf, 2019. [Online]. Available: <Go to ISI>://WOS:000604567700296.
[28] Z. Xie, O. Schwartz, A. Prasad, Decoding of finger trajectory from ECoG using deep learning, J. Neural Eng. 15 (3) (2018), https://doi.org/10.1088/1741-2552/aa9dbe.
[29] F. Ma, F. Song, Y. Liu, J. Niu, sEMG-Based Neural Network Prediction Model Selection of Gesture Fatigue and Dataset Optimization, Comput. Intell. Neurosci. 2020 (2020) 8853314, https://doi.org/10.1155/2020/8853314.
[30] F. Xiao, Y. Wang, Y. Gao, Y. Zhu, J. Zhao, Continuous estimation of joint angle from electromyography using multiple time-delayed features and random forests, Biomed. Signal Process 39 (2018) 303–311.
[31] K.J. You, K.W. Rhee, H.C. Shin, Finger Motion Decoding Using EMG Signals Corresponding Various Arm Postures, Exp. Neurobiol. 19 (1) (2010) 54–61, https://doi.org/10.5607/en.2010.19.1.54.
[32] K. Englehart, B. Hudgins, P.A. Parker, "A wavelet-based continuous classification scheme for multifunction myoelectric control," (in English), IEEE T Bio-Med. Eng. 48 (3) (2001) 302–311, https://doi.org/10.1109/10.914793.
[33] H. Qiao, T. Wang, P. Wang, S. Qiao, L. Zhang, A Time-Distributed Spatiotemporal Feature Learning Method for Machine Health Monitoring with Multi-Sensor Time Series, Sensors 18 (2018) 1–20.
[34] F.J. Ordóñez, D. Roggen, Deep Convolutional and LSTM Recurrent Neural Networks for Multimodal Wearable Activity Recognition, Sensors 16 (2016) 1–25.

Nayan M. Kakoty, IEEE Senior Member, received Bachelor's degree in Electrical Engineering, Master of Technology in Bioelectronics and PhD in the area of Rehabilitation Robotics. He worked in City University of Hong Kong as Post-Doctoral Fellow and currently working as a Professor in the department of ECE, Tezpur University, India. He is leading the Embedded Systems and Robotics Lab (www.tezu.ernet.in/erl) and his research interest is anthropomorphic prosthetic hand and co-adaptation of user with prosthesis.

Tanaya Das received her Master of Technology degree in Bioelectronics in 2021 and her Bachelor of Technology degree in Electronics and Communication Engineering in 2019 from Tezpur University, India. Her current research interests lie in the fields of deep learning, machine learning, biomedical signal processing and rehabilitation robotics.

Lakhyajit Gohain graduated from Tezpur University in 2018 with Bachelor's degree in Electronics and Communication Engineering. He pursued Masters degree in Bioelectronics with specialisation in rehabilitation robotics in 2021. Currently he is working on cloud technologies as an Infrastructure engineer at Deloitte Consulting, Bengaluru. He has worked on multiple projects associated with robotics and IoT. He has keen interest in multidisciplinary technologies and looking forward to work on the same.

MB Malarvili received the bachelor's and master's degrees in biomedical signal processing from Universiti Teknologi Malaysia (UTM), Malaysia and the Ph.D. degree in medical sciences engineering from the University of Queensland, Brisbane, Australia, in 2008. She is currently with the School of Biomedical Engineering and Health Science and the Head of the Biosignal Processing Research Group, UTM. She has authored and co-authored over 100 research papers in peer-reviewed journals, book chapters, and conference proceedings. Her research interest includes the areas of physiological signal processing, pattern recognition in biomedical applications, time-frequency signal analysis, multi-modal signal processing, computer aided medical diagnosis system, and biomedical data.

Gajendra Kumar received bachelor's degree in Human Biology, Master and PhD in Pharmacology. He worked at City University of Hong Kong and University of Illinois at Chicago, USA as a Post-Doctoral Fellow. He is currently working as Research Assistant Professor at Department of Molecular Biology, Cell Biology & Biochemistry (MCB), Brown University, USA. He investigates the novel therapeutics for neurodegenerative diseases using electrophysiology in rodents model of disease, brain computer interphase and artificial intelligence.

Prihartini Widiyanti graduated from Dentistry Faculty of Universitas Airlangga, Master of Basic Medical Sciences from Postgraduate Faculty of Universitas Airlangga and Doctoral Degree of Medical Sciences from Postgraduate Faculty Universitas Airlangga. She performed her doctoral research in Institute of Biochemistry University of Humboldt - Charite University of Clinics Berlin Germany by DAAD funding. She has performed researches in constructing diagnostic kit and anti- infectious disease in Institute of Tropical Disease Universitas Airlangga and created several artificial organs and scaffolds for Regenerative medicine. She has authored an Co-authored more than 75 reputed international journals, book chapters and international conference proceedings. Her research interest is in Biomedical sciences, Biomaterial, Tissue Engineering, Artificial Organs, Molecular Biology and Regenerative Medicine.

Hierarchical approach for fusion of electroencephalography and electromyography for predicting finger movements and kinematics using deep learning

ORIGINALITY REPORT

15%	12%	11%	0%
SIMILARITY INDEX	INTERNET SOURCES	PUBLICATIONS	STUDENT PAPERS

PRIMARY SOURCES

1	coek.info Internet Source	1%
2	www.mdpi.com Internet Source	1%
3	new.esp.org Internet Source	1%
4	Neha Hooda, Ratan Das, Neelesh Kumar. "Fusion of EEG and EMG signals for classification of unilateral foot movements", Biomedical Signal Processing and Control, 2020 Publication	1%
5	sam.ensam.eu Internet Source	<1%
6	unair-staging.elsevierpure.com Internet Source	<1%
7	diglib.tugraz.at Internet Source	<1%

8	KEIKO OGAWA. "Brain potentials associated with the onset and offset of rapid eye movement (REM) during REM sleep", Psychiatry and Clinical Neurosciences, 6/2002 Publication	<1 %
9	uu.diva-portal.org Internet Source	<1 %
10	www.scilit.net Internet Source	<1 %
11	dokumen.pub Internet Source	<1 %
12	Bhart Gupta, P. Prakasam, T. Velmurugan. "Integrated BERT embeddings, BiLSTM-BiGRU and 1-D CNN model for binary sentiment classification analysis of movie reviews", Multimedia Tools and Applications, 2022 Publication	<1 %
13	IFMBE Proceedings, 2014. Publication	<1 %
14	Lakhyajit Gohain, Krishna Sarma, Amlan Jyoti Kalita, Nayan M. Kakoty, Shyamanta M. Hazarika. "EMG controlled adaptive multi-grasp prosthetic hand with an android interface", International Journal of Intelligent Robotics and Applications, 2022 Publication	<1 %

15	Wei Tang, Fazhi He, Yu Liu. "TCCFusion: An infrared and visible image fusion method based on transformer and cross correlation", Pattern Recognition, 2023 Publication	<1 %
16	arxiv.org Internet Source	<1 %
17	eprints.gla.ac.uk Internet Source	<1 %
18	www.nature.com Internet Source	<1 %
19	Kiat Hui Khng, Ravikiran Mane. "Beyond BCI—Validating a wireless, consumer-grade EEG headset against a medical-grade system for evaluating EEG effects of a test anxiety intervention in school", Advanced Engineering Informatics, 2020 Publication	<1 %
20	fsktm.um.edu.my Internet Source	<1 %
21	link.springer.com Internet Source	<1 %
22	stdj.scienceandtechnology.com.vn Internet Source	<1 %
23	www.atlantis-press.com Internet Source	<1 %

24	bc.pollub.pl Internet Source	<1 %
25	pubmed.ncbi.nlm.nih.gov Internet Source	<1 %
26	sci-hub.se Internet Source	<1 %
27	www.biorxiv.org Internet Source	<1 %
28	Ling Yu, Jin Chen, Guoru Ding. "Spectrum prediction via long short term memory", 2017 3rd IEEE International Conference on Computer and Communications (ICCC), 2017 Publication	<1 %
29	www.deepdyve.com Internet Source	<1 %
30	anavara.com Internet Source	<1 %
31	kyutech.repo.nii.ac.jp Internet Source	<1 %
32	watermark.silverchair.com Internet Source	<1 %
33	www.cs.utah.edu Internet Source	<1 %
34	academic.oup.com Internet Source	<1 %

35	assets.researchsquare.com Internet Source	<1 %
36	digitalcommons.unl.edu Internet Source	<1 %
37	"Frontier Computing", Springer Science and Business Media LLC, 2020 Publication	<1 %
38	Manalee Dev Sharma, Nabasmita Phukan, Nayan M. Kakoty, Durlav Sonowal. "Visualization of Grasping Operations based on Hand Kinematics measured through Data Glove", Proceedings of the Advances in Robotics on - AIR '17, 2017 Publication	<1 %
39	journals.iium.edu.my Internet Source	<1 %
40	prod-dcd-datasets-public-files-eu-west-1.s3.eu-west-1.amazonaws.com Internet Source	<1 %
41	sibran.ru Internet Source	<1 %
42	Meihua Wang, Chao Li, Fanhui Ke. "Recurrent multi-level residual and global attention network for single image deraining", Neural Computing and Applications, 2022 Publication	<1 %

43	answerpot.com Internet Source	<1 %
44	ijcttjournal.org Internet Source	<1 %
45	sersc.org Internet Source	<1 %
46	www.advancesinrobotics.com Internet Source	<1 %
47	www.tcsae.org Internet Source	<1 %
48	"Advances in Service and Industrial Robotics", Springer Science and Business Media LLC, 2019 Publication	<1 %
49	"Converging Clinical and Engineering Research on Neurorehabilitation II", Springer Nature, 2017 Publication	<1 %
50	pdfs.semanticscholar.org Internet Source	<1 %
51	www.nsf.gov Internet Source	<1 %
52	www.slideshare.net Internet Source	<1 %
	backoffice.biblio.ugent.be	

53	Internet Source	<1%
54	cs229.stanford.edu Internet Source	<1%
55	int-jecse.net Internet Source	<1%
56	os.zhdk.cloud.switch.ch Internet Source	<1%
57	summit.sfu.ca Internet Source	<1%
58	www.actabio.pwr.wroc.pl Internet Source	<1%
59	www.sfn.org Internet Source	<1%
60	"Advances in Communication, Devices and Networking", Springer Science and Business Media LLC, 2023 Publication	<1%
61	"Advances in Computational Intelligence", Springer Science and Business Media LLC, 2021 Publication	<1%
62	"Intelligent Systems Design and Applications", Springer Science and Business Media LLC, 2020 Publication	<1%

63	"Recent Advances on Soft Computing and Data Mining", Springer Science and Business Media LLC, 2017 Publication	<1 %
64	E Safari, D.L Hopkins, N.M Fogarty. "Diverse lamb genotypes 4. Predicting the yield of saleable meat and high value trimmed cuts from carcass measurements", Meat Science, 2001 Publication	<1 %
65	Nayan M. Kakoty, Lakhyajit Gohain, Juri Borborua Saikia, Amlan Jyoti Kalita, Satyajit Borah. "Real-time EMG based prosthetic hand controller realizing neuromuscular constraint", International Journal of Intelligent Robotics and Applications, 2022 Publication	<1 %
66	Pei-Chi Hsiao, Shu-Yu Yang, Bor-Shing Lin, I-Jung Lee, Willy Chou. "Data glove embedded with 9-axis IMU and force sensing sensors for evaluation of hand function", 2015 37th Annual International Conference of the IEEE Engineering in Medicine and Biology Society (EMBC), 2015 Publication	<1 %
67	Tarek M. Bittibssi, Abdelhalim Zekry, Mohamed A. Genedy, Shady A. Maged. "Implementation of surface electromyography	<1 %

controlled prosthetics limb based on recurrent neural network", Concurrency and Computation: Practice and Experience, 2022
Publication

68	downloads.hindawi.com Internet Source	<1 %
69	mafiadoc.com Internet Source	<1 %
70	ouci.dntb.gov.ua Internet Source	<1 %
71	psecommunity.org Internet Source	<1 %
72	ro.uow.edu.au Internet Source	<1 %
73	www.escholar.manchester.ac.uk Internet Source	<1 %
74	www.journalofdairyscience.org Internet Source	<1 %
75	www.pure.ed.ac.uk Internet Source	<1 %
76	xml.thinkonweb.com Internet Source	<1 %
77	Sanjay Kumar Dwivedi, Jimson Ngeo, Tomohiro Shibata. "Extraction of Nonlinear Synergies for Proportional and Simultaneous	<1 %

Estimation of Finger Kinematics", IEEE Transactions on Biomedical Engineering, 2020
Publication

---

78 A. Costa-García, E. Iáñez, A.J. del-Ama, A. Gil-Agudo, J.M. Azorín. "EEG model stability and online decoding of attentional demand during gait using gamma band features", Neurocomputing, 2019 <1 %
Publication

---

79 M.A. Ahmed, B.B. Zaidan, A.A. Zaidan, Mahmood M. Salih, Z.T. Al-qaysi, A.H. Alamoodi. "Based on wearable sensory device in 3D-printed humanoid: A new real-time sign language recognition system", Measurement, 2021 <1 %
Publication

---

80 Nishant Ganesh Kumar, Theodore A. Kung, Paul S. Cederna. "Regenerative Peripheral Nerve Interfaces for Advanced Control of Upper Extremity Prosthetic Devices", Hand Clinics, 2021 <1 %
Publication

---

81 Xiangxu Deng, Shu Zhang, Jun Wang, Ken Chen. "Chapter 27 Named Entity Recognition of Wa Cultural Information Resources Based on Attention Mechanism", Springer Science and Business Media LLC, 2021 <1 %
Publication

82	spiral.imperial.ac.uk Internet Source	<1%

Exclude quotes	On	Exclude matches	< 5 words
Exclude bibliography	On		

Hierarchical approach for fusion of electroencephalography and electromyography for predicting finger movements and kinematics using deep learning

GRADEMARK REPORT

FINAL GRADE

/0

GENERAL COMMENTS

Instructor

PAGE 1

PAGE 2

PAGE 3

PAGE 4

PAGE 5

PAGE 6

PAGE 7

PAGE 8

PAGE 9

PAGE 10

PAGE 11

PAGE 12